

# Meteorology Visibility Estimation by Using Multi-Support Vector Regression Method

Wai Lun Lo, Meimei Zhu, and Hong Fu

Department of Computer Science, Chu Hai College of Higher Education, 80 Castle Peak Road, Castle Peak Bay, Tuen Mun, N.T. Hong Kong

Email: {wlo, mayzhu, hfu}@chuhai.edu.hk

**Abstract**—Meteorological visibility measures the transparency of the atmosphere or air and it provides important information for road, flight and sea transportation safety. Problem of pollution can also affect the visibility of a certain area. Measurement and estimation of visibility is a challenging and complex problem as visibility is affected by various factors such as dust, smoke, fog and haze. Traditional digital image-based approach for visibility estimation involve applications of the meteorology law and mathematical analysis. Digital image-based and machine learning approach can be one of the solutions to this complex problem. In this paper, we propose an intelligent digital method for visibility estimation. Effective regions are first extracted from the digital images and then classified into different classes by using Support Vector Machines (SVM). Multi-Supported Vector Regression (MSVR) models are used to predict the meteorological visibility by using the image features values generated by VGG Neural Network. SVR machine learning method is used for model training and the resulting system can be used for meteorological visibility estimation.

**Index Terms**—meteorology visibility, weather photo, deep learning, feature extraction, support vector regression

## I. INTRODUCTION

Meteorological Visibility is a measure of the distance at which an object can be clearly discerned. Visibility refers to transparency of air and is reported within surface weather observations. In general, visibility affects different forms of traffic including roads, sea and aviation. Visibility can be represented in two ways: (1) the greatest distance at which an object situated near the ground can be seen and recognized in a bright background. It is represented by the meteorological optical range or (2) the greatest distance at which lights of 1,000 candelas can be identified in unlit background and this measurement varies with background illumination. These two measurements have different values in air of a given extinction coefficient. Visibility can be as high as hundreds of kilometers under extremely clean air weather conditions. However, visibility can be reduced by air pollution and high humidity. Under the conditions of very low or nearly zero visibility that is due to fog and smoke, driving is extremely dangerous. The same can happen

near desert areas, when there is sandstorm, or forest fires. Heavy rain, blizzards and blowing snow also causes low visibility.

Low visibility conditions with less than 100m is usually reported as zero. In this case, road may be closed and automatic warning signs may be activated in order to give warnings to road drivers. This is an important follow-up actions for certain area that are affected by repeatedly low visibility. Visibility readings are often issued by the government weather agency. The government weather agency will advise drivers to avoid travel until the weathers' conditions improve. Visibility also affects the aviation, airport travel is also often delayed due to low visibility as moving aircraft on ground or landing is difficult or even dangerous under this low visibility conditions. In Hong Kong, visibility readings are announced to public by the Hong Kong Observatory (HKO).

One of the apparent symptoms of air pollution is the reduction of visibility. Absorption and scattering of light by particles and gases in the atmosphere will caused visibility degradation. Scattering particulates impairs visibility readily. Visibility is reduced by significant scattering from particles between an observer and a distant object. Through the line of sight from observer to an object, the particles scatter light from the sun and the rest of the sky. Such effect will decrease the contrast between the object and the background sky. Particles with diameter in the range of 0.1-1.0 $\mu$ m mostly affect and reduce the visibility and these particles can be due to air pollution.

Monitoring of visibility not only provides judgment for whether the weather conditions are safe for road, air and sea transport but also provide information for air pollution. For the existing practice in Hong Kong, the visibility is officially reported by the Hong Kong Observatory every day by using a sophisticated and high cost specialized equipment and human experts' judgment. For the research of environmental parameters monitoring. The major objectives of this research project is to investigate the problem of visibility estimation by using digital image processing and artificial intelligence algorithms, and to develop a Visibility Estimation system with relative low cost equipment and reasonable accuracy. It is expected that the proposed system can operate and monitor the visibility automatically. The outcomes of this research project can provide an intelligent visibility

estimation method for the purpose of environmental parameters monitoring and contribute to the research area of sustainability technology.

Monitoring visibility can be mainly classified into the following approaches: (1) visual observation by trained meteorological observers, (2) optical measurement by visibility meter (3) digital evaluation on camera image.

For the first method, trained experts will generally ignore the noise caused by different weather conditions. By recognizing the natural or man-made targets as landmark targets at the greatest distance, the trained experts can estimate the meteorological optical range (MOR) by human judgment. Number of reference targets in the observation environment, the contrast determination based on observer's vision and the limit of human feelings can affect the results of visual method. In normal practice, visibility observation can just be conducted hourly and that will cause a quite long time for visibility verification. Tall buildings in the city due to city development will become obstacles to distant scene or objects. All the above factors will affect the results of Visual method.

Visibility measurement by using optical visibility meter is also one of the most popular methods in automatic visibility measurement. By using optical sensors to measure the length of atmosphere over which a beam of light travels before luminous flux reduced to 5% of original value, the visibility meter can measure the light extinction to estimate the meteorological optical range. Visibility meter designs includes transmission method, forward-scatter method and backscatter method. In Forward-scatter method, the meter measures a small portion of light scattered out of a light beam to estimate the extinction coefficient. Forward-scatter method is the most widely used in automatic visibility measurement in terms of sensitivity, correctness, compactness and price. However, this equipment in general is very expensive and needs high installation requirements. It can just measure a short path of the atmosphere, so the accuracy is limited.

Camera-based visibility monitoring techniques is a relative low cost method and has been widely used to estimate the visibility in the past [1]-[15]. Camera-based method can be mainly divided into three classes: (1) Road transportation based on road camera [1]-[5] (2) Reference method corresponding to visual method (3) Applications of law in meteorology [7]-[15].

In the first method of road transportation based on road camera [1]-[5], the special references on road such as the straight road or the road marks, are used to calculate the meteorological optical range. This approach is used for low visibility on road as the road camera just contains the road scene within a relatively short distance. For the second image method which is corresponding to visual method, visible targets are provided in the panorama and the visibility is evaluated by detecting whether or not the edge of targets is visible [6]. Sufficient number of targets is needed in order to get a better measurement range and accuracy.

The third image method is based on the law in meteorology such as Koschmieder equation or Lambert-

beer law [7]-[15] for the analysis of visibility. Based on the meteorological law, features related to the extinction coefficient or visibility distance are extracted from the image to evaluate the visibility. In the past research, a physics-based model to express the mapping between the contrast and the atmospheric visibility distance with the consideration of Lambertian surfaces of the scene was proposed [7]-[9]. Two tree sets located at different but known distances are used to calculate the extinction coefficient based on the different wavelengths associated with R,G,B channels of the image [10] from which visibility can be estimated. In digital image method, the image quality and reference targets are both important for feature extraction and visibility evaluation. As image quality and contrast are affected by many factors including light source, weather condition and camera setting. It is difficult to extract all the related features to describe the complex effect of the factors on visibility. Computer vision-based visibility estimation is one of the popular research topics in the past [16]-[19].

In this paper, a Multi-SVR Models Learning Method for visibility estimation will be proposed. The effective regions are then extracted from the digital images with different landmark indicators. From the image data of the effective regions, image features of the digital images are extracted by the VGG16 Neural Network [20] and this feature dataset will be classified into different class by using a Support Vector Machines (SVM) [21]-[28]. Multi-Support Vector regression models (MSVR) will be trained to build the models that correlates the VGG16 image features with the visibility. Trained MSVR models can then be used for visibility estimation with digital image of the selected site are fed as input to the MSVR models. The paper is organized as follows. The construction of the visibility image database is described in Section II. The proposed System Architecture and the methodology are described in Section III. The simulation results and the comparison with other algorithms are discussed in Section IV and Section V respectively while a final conclusion will be given in Section VI.

## II. VISIBILITY IMAGE DATABASE CONSTRUCTION

In this paper, training and testing of the proposed algorithm in this paper is based on a digital image dataset provided by the Hong Kong Observatory for the period from Feb 2019 to Mar 2019.

### A. Visibility Report by HKO

Visibility readings in Hong Kong Waters are available in official web site of the Hong Kong Observatory (HKO) and these readings are considered as ground truth for the evaluation of the performance of the proposed algorithm in this paper. The HKO web site provides a visibility readings map for the public reference (Fig. 1). An example of visibility readings map of the Hong Kong Waters is shown in Fig. 1. The map consists of visibility readings in Hong Kong Waters at the indicated hour. All these readings are provided by the Hong Kong Observatory (HKO) and Marine Department respectively. The HKO provides visibility readings for several site in

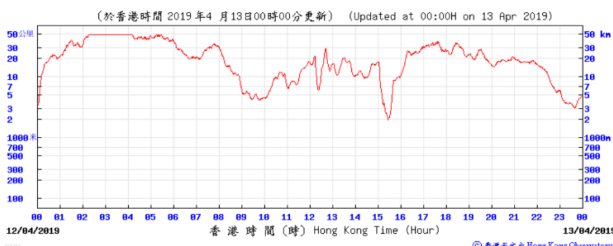
Hong Kong. The visibility readings for Hong Kong Observatory are based on hourly observations by a trained meteorological observer. While the visibility readings at Chek Lap Kok, Central, Sai Wan Ho and Waglan Island are derived from automatic visibility readings of a visibility meter and all these readings are the average of readings in the 10 minutes ending at the indicated time. Other readings in the map are collected by the Marine Department. The visibility readings provided by HKO are in the range between 100m and 50 km. Visibility report of 100m represents visibilities of 100m or less and, while 50km refers to visibilities of 50km or more.



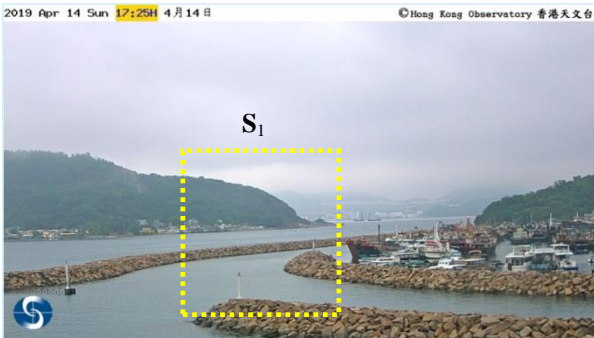
Figure 1. Visibility readings in Hong Kong Waters 9 Apr 2019 [29]

### B. Weather Photos and Visibility Readings Dataset

The Hong Kong Observatory takes weather photos at 28 selected site in Hong Kong. These photos are taken automatically in every 5 minutes and low-resolution weather photos are released to public on the HKO official website [29]. Visibility readings at selected site in Hong Kong are also reported in the HKO official website in which visibility readings at five selected sites Chek Lap Kok, Central, Hong Kong Observatory, Sai Wan HO and Waglan Island are reported. An example of visibility curve at Sai Wan Ho is shown in Fig. 2.



(a) An example of visibility readings at Sai Wan HO



(b) Weather photo at Sai Wan Ho



(c) Landmark of selected site Sai Wan Ho in (b)

Figure 2. Visibility curve and weather photos at selected site (\*From HKO website: <http://www.hko.org.hk>)

Past research has been done based on analyzing the image features of the low-resolution webcam weather photos given by HKO website [30], the prediction accuracy can reach 62%. In contrast to the past research in [30] which uses webcam photos for visibility estimation, the image dataset and visibility readings for the simulation studies in this paper are provided by the Hong Kong Observatory. In this paper, the site Sai Wan Ho is selected as a case for the simulation studies in this paper. An example of weather photo and its landmark indicators are shown in Fig. 2. The digital image dataset provided by the Hong Kong Observatory consists of weather photos and visibility readings for the period from Feb 2019 to Mar 2019. The weather photos are sorted in ascending order of visibility readings. The dataset is then divided into 5 subgroups for different visibility reading ranges (Table I) and leave-one-out approach is used to train the SVM and SVRs.

### C. Review of Supported Vector Regression

It is well known that past research on SVM has been done for classification of image objects [21]-[28] and SVR has been developed for mapping data set [21]-[28] by a non-linear regression function  $y=f(\mathbf{x})$ . A brief summary of the SVR method is as follows.

1. Define a nonlinear regression mapping  $\varphi(\mathbf{x}): \mathbf{R}^n \rightarrow \mathbf{R}^m$  to map the training set  $\{(\mathbf{x}_i, y_i)\}_{i=1}^N$  into feature space  $\mathbf{R}^m$
2. Transform the nonlinear regression problem in low-dimensional feature space into a linear problem by a linear SVR function  $f(\mathbf{x})$  in high-dimensional space

$$f(\mathbf{x}) = \mathbf{w}^T \varphi(\mathbf{x}) + b$$

where  $f(\mathbf{x})$  is the predicted values and the coefficients  $\mathbf{w}$  ( $\mathbf{w} \in \mathbf{R}^m$ ) and  $b$  ( $b \in \mathbf{R}$ ) are adjustable

3. Define the risk function  $R_r(\mathbf{f})$ ,

$$R_r(\mathbf{f}) = \frac{1}{N} \sum_{i=1}^N \Theta_\varepsilon(y_i, \mathbf{w}^T \varphi(\mathbf{x}_i) + b)$$

where is the  $\varepsilon$ -intensive loss function

$$\Theta_\varepsilon(y, f(\mathbf{x})) = \begin{cases} |f(\mathbf{x}) - y| - \varepsilon & \text{if } |f(\mathbf{x}) - y| \geq \varepsilon \\ 0 & \text{otherwise} \end{cases}$$

The  $\varepsilon$ -intensive loss function is used to control the sparsity of the solutions and the generalization of the models.

- Determine the overall training error between the training data and the  $\varepsilon$ -intensive loss function for the following quadratic optimization problem with inequality constraints.

$$\text{Min}_{w,b,\xi,\xi^*} R_\varepsilon(w, \xi^*, \xi) = \frac{1}{2} w^T w + C \sum_{i=1}^N (\xi_i + \xi_i^*)$$

$$\text{Subject to } y_i - \mathbf{w}^T \varphi(\mathbf{x}_i) - b \leq \varepsilon + \xi_i^*, \quad i=1,2,\dots,N$$

$$\mathbf{w}^T \varphi(\mathbf{x}_i) - y_i + b \leq \varepsilon + \xi_i, \quad i=1,2,\dots,N$$

$$\xi_i^*, \xi_i \geq 0, \quad i=1,2,\dots,N$$

First term is used to penalize large weights. The second term is used to penalize training error and C is a parameter to balance these 2 terms. The training errors below  $-\varepsilon$  are represented as  $\xi_i$ , otherwise they are represented as  $\xi_i^*$ .

- Solve the quadratic optimization problem to derive the parameter vector  $\mathbf{w}$  in step 4.

$$w = \sum_{i=1}^N (\beta_i^* - \beta_i) \varphi(x_i)$$

where  $\beta_1^*$  and  $\beta_1$  are the Lagrangian multipliers

- The SVR regression function is then given by:

$$f(x) = \sum_{i=1}^N (\beta_i^* - \beta_i) K(x_i, x_j) + b$$

$$K(x_i, x_j) = \exp(-\lambda \|x_i - x_j\|^2), \quad \lambda > 0$$

where  $K(\mathbf{x}_i, \mathbf{x}_j) = \varphi(\mathbf{x}_i) \circ \varphi(\mathbf{x}_j)$  is the kernel function and radial basis function (RBF) is selected as kernel function for nonlinear mapping of training dataset.

#### D. Visibility Readings and Digital Image Dataset

The weather photos with dimension of 1280 x 760 and visibility readings from Feb 2019 to Mar 2019 have been collected and this data covers the visibility ranges from 0 km to 50 km. The visibility data distribution is summarized in Table I.

TABLE I. VISIBILITY DATA DISTRIBUTION

Range of Visibility	No. of Samples	Percentage (%)
0-10 km	210	25.64
10-20 km	404	49.33
20-30 km	73	8.91
30-40 km	65	7.94
40-50 km	67	8.18

### III. METHODOLOGY

#### A. Review of Classical Approach

Classical approach for visibility estimation involves the uses of the theory of the apparent luminance of objects against background sky. Meteorological law such as Koschmieder equation and Lambert-beer law can be used for estimation of extinction coefficient of the atmosphere and the visibility of atmosphere. The apparent luminance  $I$  of an object is given by:

$$I = I_0 e^{-kd} + I_b (1 - e^{-kd}) \quad (1)$$

where  $k$  is the extinction coefficient,  $I_b$  is the luminance of the sky;  $I_0$  and  $d$  are the intrinsic luminance and the distance of the object, respectively. Then Lambert-beer law is further proposed to estimate the extinction coefficient, which is an attenuation law of atmospheric contrasts:

$$C = C_0 e^{-kd} \text{ and } C = \frac{I_b - I}{I_b} \quad (2)$$

$C$  and  $C_0$  are the apparent contrast at distance  $d$ . For a contrast threshold of 0.05, if  $C_0=1$ , the meteorological visibility distance  $V_{met}$  can be estimated by  $V_{net} \cong 3/k$ . However, the accuracy of the classical approach is affected by a number of factors such as luminance of image, the cloud, the location of sun, dust, smoke, fog, haze and so on. Therefore, we propose to extract the image features by using the VGG16 neural network which can provide information for the complex characteristics of a digital image.

#### B. Proposed Multi-SVR System for Visibility Estimation

A block diagram for the proposed system is shown Fig. 4. Effective image regions  $\mathbf{S}_i$  are extracted from the digital image  $\mathbf{D}_i$  according to pre-requisite distance information of the landmark objects. The effective regions  $\mathbf{S}_i$  will then be passed to a VGG16 network for generation of image features. The feature vectors  $\mathbf{X}$  will be passed into a Support Vector Machine (SVM) [22] from which we can derived the class  $\mathbf{C}_i$  of the regions. Each class refers to different ranges of visibility readings. The feature vector  $\mathbf{X}$  is then passed to the corresponding Support Vector Regression (SVR) models for visibility estimation.

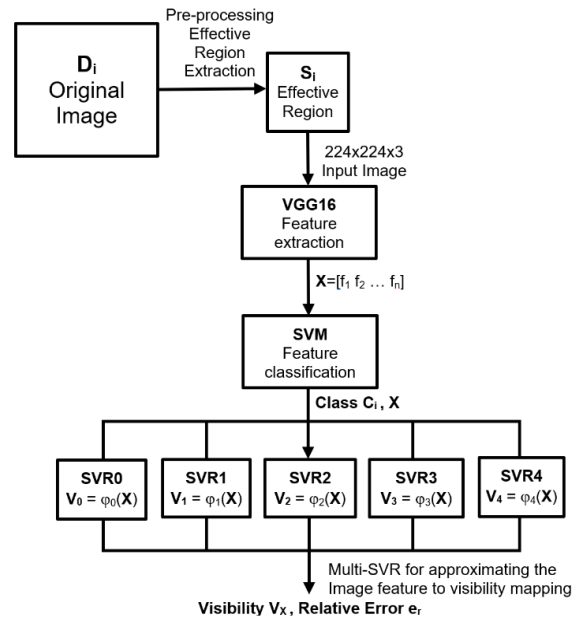


Figure 3. Proposed multi-SVR system

#### C. Image Pre-processing and Effective Region Extraction

As shown in Fig. 2, digital image can be divided into image regions with different landmark objects. Consider

the case of a selected image region  $S_i$  containing a landmark object at  $D_m$  from the observing point. For visibility readings larger than  $D_m$ , we can expect that clear landmark object can be seen in the image region. However, as visibility falls near to  $D_m$ , there will be variations in the image content of the landmark object. The contrast between the landmark object and the surrounding will be reduced and the landmark object will disappear when visibility fall below  $D_m$ . This situation is similar to the case of estimating visibility by a trained meteorological observer. Landmark objects will show image content variation when visibility readings fall near to the distance range of the landmark object.

After extensive simulation studies, it has been found that image region without landmark objects in the distance range of interested cannot provide sufficient information for data model training and accurate visibility estimation. Effective Regions should cover landmark objects for different visibility ranges. Therefore, we propose to estimate visibility by observing the image features of appropriate effective region  $S_i$  based on the pre-requisite distance information of landmark objects. In this paper we have test the algorithms for 5 cases of effective regions. An example of effective region  $S_1$  is shown in Fig. 2.

#### D. Image Feature Extraction

Having extracted the effective image regions  $S_i$ , the digital image data of the regions are passed into the pre-trained VGG16 Neural Network (NN) [20] for generating image feature vector  $\mathbf{X}$ . The structure of VGG16 [20] is shown in Fig. 4. In this paper, we have tested the feature values at different layers of VGG16 for visibility estimation. It has been found that the feature values at output layer (dimension 1000) is most effective for visibility estimation. The feature vectors  $\mathbf{X}=[f_1 f_2 \dots f_L]$  generated by the VGG16 output layer is used for SVM and SVR training. Samples of filtered image data at the output layer of the VGG16 network are shown in Fig. 5.

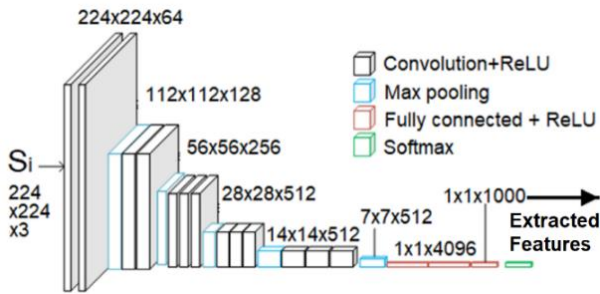
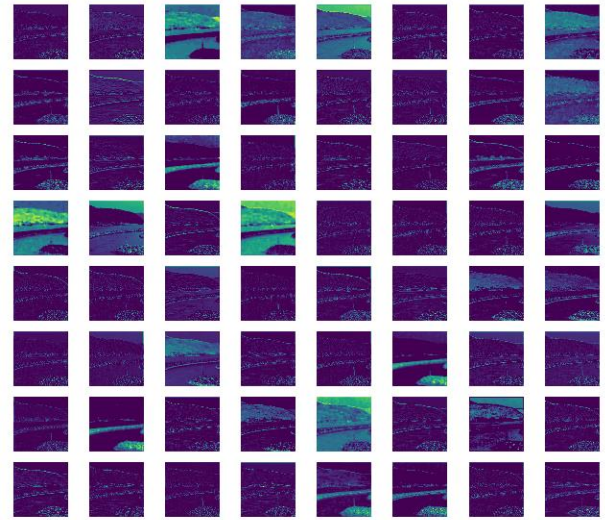
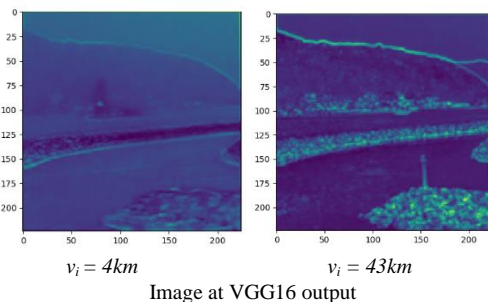


Figure 4. Architecture of VGG16 network



VGG16 filtered image at internodes with  $v_i = 43km$

Figure 5. VGG16 filtered image

#### E. SVM for Image Classifications

The feature vectors  $\mathbf{X}$  are then classified into classes with different visibility ranges. The classes for different visibility ranges are summarized in the following Table II. As shown in Fig. 2, the SVM is trained according to the training dataset of  $\mathbf{X}$  for different visibility ranges. All parameters for the SVM training algorithms are default values. In order to ensure the continuity of estimation ranges, there are overlapping regions between different  $C_i$  classes as shown in Table II.

TABLE II. VISIBILITY CLASSES  $\delta = 4km$

Class	Visibility Range
$C_0$	0-12 km
$C_1$	8-22 km
$C_2$	18-32 km
$C_3$	28-42 km
$C_4$	38-50 km

#### F. Multi-SVR Regression Models for Visibility Estimation

After obtaining the class  $C_i$  of the feature vector  $\mathbf{X}$ , the feature vectors will be passed to the corresponding SVR model for data training. The parameter  $C$  is a penalty factor that reflects the degree to which the model penalizes the sample data. If  $C$  is too large, the generalization ability of the model is poor. If  $C$  is too small, the model error is large. The value of  $C$  is determined according to the specific experiment. In this paper, the  $C$  value is 100. Common kernel functions include linear kernel function, polynomial kernel function and Gaussian radial basis kernel function. In this paper, Gaussian radial basis kernel function is used for SVR modeling. As shown in Fig. 3, five SVR models are connected in parallel. Each SVR model is designed for a specific visibility range. The objective of SVR training is to tune the SVR models so that the overall multi-parallel SVR models can approximate the nonlinear mapping between the feature vectors  $\mathbf{x}=[f_1 f_2 \dots f_L]$  and the visibility  $v_x = \varphi_i(\mathbf{x})$  for different classes ( $C_1, C_2, \dots, C_5$ ) of  $\mathbf{X}$ .

After extensive training of SVR models, the overall multi-SVR models can be used to estimate visibility based on the digital image data  $D_i$ .

IV. SIMULATION STUDIES AND COMPARISON

In order to evaluate the performances of the proposed algorithms, simulation studies have been conducted and the results are summarized in Table III-Table V. In Table III,  $N[V_i^*]$  is the predicted values and  $N[V_i]$  is the expected values. In Table IV, we use the SVR relative percentage error  $e_r$  for performance evaluation,

$$e_r = \frac{1}{N} \sum_{i=1}^N \frac{|V_i^* - \hat{V}_i|}{V_i^*}$$

The overall average  $e_r$  for all the cases is 12.15%. About 85% of the predicted values are matched with the expected values as shown in Fig. 6. The number of visibility class is selected to be 5 and this parameter is a compromise between prediction accuracy and computation complexity. Simulation results shows that 5 visibility classes can give prediction accuracy about 85%. As compared to the past research work of [30] in which the prediction accuracy is about 62%. The simulation results for different selection of effective image regions  $S_i$  ( $i=1..5$ ) are summarized in Table V and Fig. 6.  $S_5$  is the whole image with compression and  $S_6$  is the effective region for the site in [30]. The performance of the proposed algorithm has been compared with the algorithm in [30]. The prediction accuracy of the algorithm in [30] for  $S_6$  is 62% while the prediction accuracy of the proposed algorithm for  $S_6$  is 83.4%. The proposed algorithm in this paper give a better performance than that of the algorithm in [30] and the Neural Network estimation method by using the hand-crafted feature vectors. Since the mapping between the image features vectors and the visibility readings is a high-dimensional complex non-linear function. Using multi-SVR models is similar to the case of approximating the complex non-linear function by a piecewise function which consists of a number of linear (or simple non-linear) function segments for different local region. From the simulation studies, combining a number of local linear function segments can give better estimation accuracy as compared to the algorithms developed in [30]. According to the simulation results, the piece wise strategy makes the result better than that in [30]. A simple linear regression is not suitable for this non-linear problem with more than one input variable.

TABLE III. NO. OF THE PREDICTED DATA & EXPECTED DATA

$N[V_i]$	$N[V_i^*]$				
	Class C <sub>0</sub>	Class C <sub>1</sub>	Class C <sub>2</sub>	Class C <sub>3</sub>	Class C <sub>4</sub>
C <sub>0</sub>	203	7	7	0	0
C <sub>1</sub>	16	318	6	1	3
C <sub>2</sub>	1	18	43	9	2
C <sub>3</sub>	0	4	8	42	11
C <sub>4</sub>	0	8	0	6	53

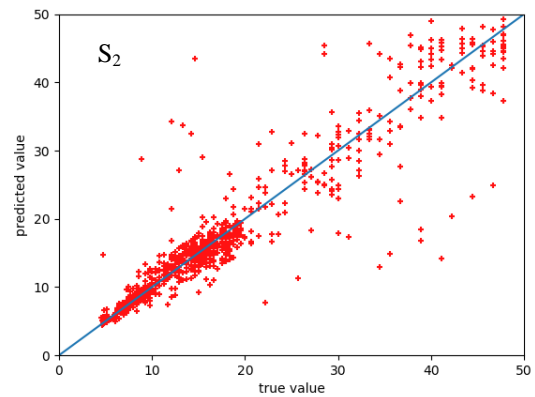
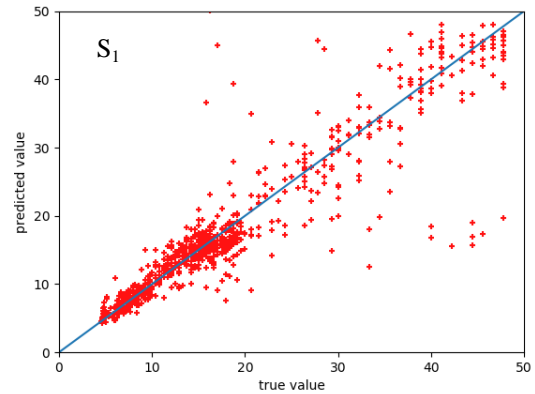
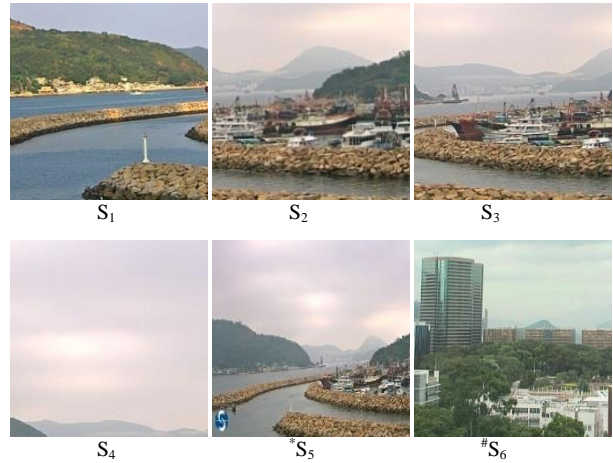
TABLE IV. NO. OF THE PREDICTED DATA & EXPECTED DATA

Visibility Range [km]	0-12	8-22	18-32	28-42	38-50
No of Samples	258	501	139	99	78
SVR $e_r$	10.03%	11.41%	10.25%	6.61%	5.51%

TABLE V. ESTIMATION ERROR FOR DIFFERENT REGIONS

Region	$S_1$	$S_2$	$S_3$	$S_4$	* $S_5$	# $S_6$
SVR $e_r$	12.15%	11.4%	11.94%	10.38%	12.22%	12.26%

\* $S_5$  is the whole image, # $S_6$  for comparison with performance of [18]



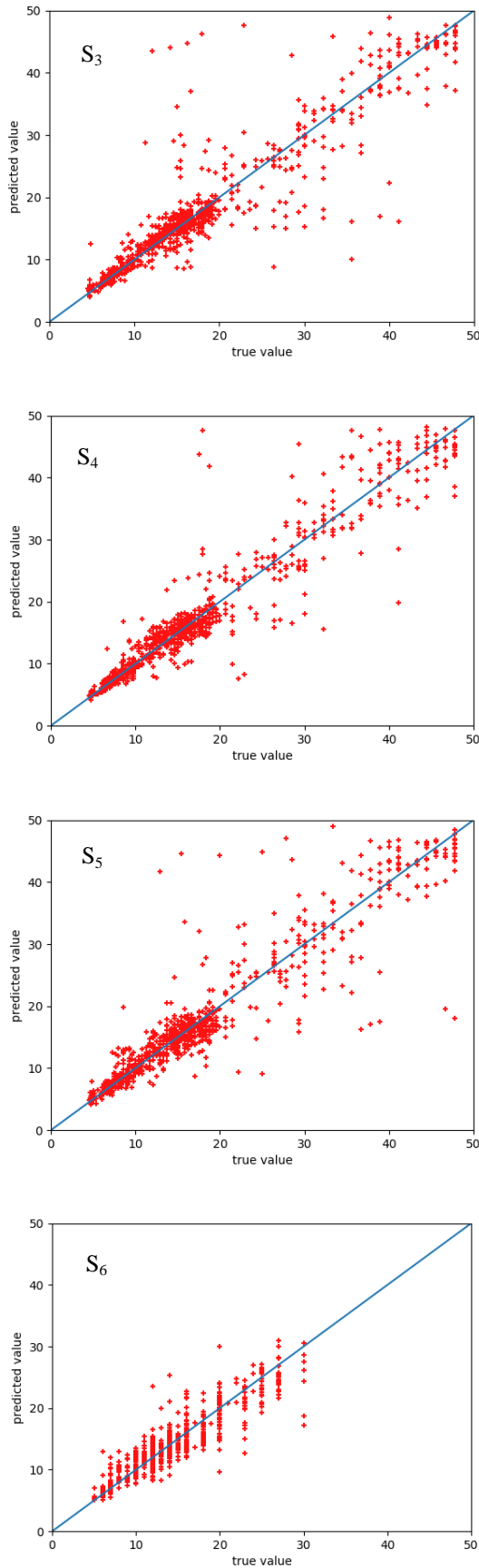


Figure 6. Scatter plot of actual and predicted visibility (km).

## V. EFFECT OF CLASSES OVERLAPPING WIDTH

In this paper, we have conducted simulation studies to evaluate the effect of overlapping width ( $\delta$ ) of visibility classes. The results are shown in Table VI.

TABLE VI. EFFECT OF SELECTION OF  $\delta$

$\delta$	Percentage Error
4km	12.57%
3km	12.28%
2km	12.15%
1km	12.21%

## VI. CONCLUSION

In this paper, a Multi-SVR visibility estimation algorithm is proposed. The generation of feature vector is based on an effective image region with size of 224x224x3 and the training of SVM and SVR are based on a relative low dimension feature vector of size 1000. The proposed algorithm can classify the effective image regions into different visibility ranges and the prediction error can be less than 12.6%. The proposed algorithm gives better performance than the Deep Learning Neural Network approach in [30].

## CONFLICT OF INTEREST

The authors declare no conflict of interest.

## AUTHOR CONTRIBUTIONS

W.L. Lo designed the algorithms, analyzed the data and prepared the paper. M. Zhu implemented the algorithms and carried out computer simulations to obtain the data and results. H. Fu designed the algorithms, analyzed the data and reviewed the paper.

## ACKNOWLEDGMENT

The work described in this paper was fully supported by a grant from the Research Grants Council of the Hong Kong Special Administrative Region, China (Project Reference No.: UGC/FDS13/E02/18). The authors would also like to thank Hong Kong Observatory for the providing the weather photos and visibility database.

## REFERENCES

- [1] N. Hautière, J. P. Tarel, J. Lavenant, and D. Aubert, "Automatic fog detection and estimation of visibility distance through use of an onboard camera," *Machine Vision and Applications*, vol. 17, no. 1, pp. 8-20, 2006.
- [2] N. Hautière, D. Aubert, É. Dumont, and J. P. Tarel, "Experimental validation of dedicated methods to in-vehicle estimation of atmospheric visibility distance," *IEEE Transactions on Instrumentation and Measurement*, vol. 57, no. 10, pp. 2218-2225, 2008.
- [3] N. Hautière and A. Boubezoul, "Combination of roadside and in-vehicle sensors for extensive visibility range monitoring," in *Proc. Sixth IEEE International Conference on Advanced Video and Signal Based Surveillance*, September 2009, pp. 388-393.
- [4] Z. Z. Chen, J. Li, and Q. M. Chen, "Real-time video detection of road visibility conditions," in *Proc. WRI World Congress on Computer Science and Information Engineering*, March 2009, vol. 5, pp. 472-476.

- [5] M. Negru and S. Nedevschi, "Image based fog detection and visibility estimation for driving assistance systems," in *Proc. IEEE International Conference on Intelligent Computer Communication and Processing*, September 2013, pp. 163-168.
- [6] D. Bäumer, S. Versick, and B. Vogel, "Determination of the visibility using a digital panorama camera," *Atmospheric Environment*, vol. 42, no. 11, pp. 2593-2602, 2008.
- [7] R. Babari, N. Hautiere, E. Dumont, R. Brémond, and N. Paparoditis, "A model-driven approach to estimate atmospheric visibility with ordinary cameras," *Atmospheric Environment*, vol. 45, no. 30, pp. 5316-5324, 2011.
- [8] R. Babari, N. Hautière, É. Dumont, N. Paparoditis, and J. Misener, "Visibility monitoring using conventional roadside cameras—Emerging applications," *Transportation Research Part C: Emerging Technologies*, vol. 22, pp. 17-28, 2012.
- [9] R. Babari, N. Hautière, E. Dumont, J. P. Papelard, and N. Paparoditis, "Computer vision for the remote sensing of atmospheric visibility," in *Proc. IEEE International Conference on Computer Vision Workshops (ICCV Workshops)*, November 2011, pp. 219-226.
- [10] F. Carretas, F. Wagner, and F. M. Janeiro, "Atmospheric visibility and Angström exponent measurements through digital photography," *Measurement*, vol. 64, pp. 147-156, 2015.
- [11] K. W. Kim, "Estimation of visibility using a visual image," *Environmental Monitoring and Assessment*, vol. 187, no. 3, pp. 1-10, 2015.
- [12] J. Wang, X. Liu, X. Yang, M. Lei, S. Ruan, K. Nie, Y. Miao, and J. Liu, "Development and evaluation of a new digital photography visiometer system for automated visibility observation," *Atmospheric Environment*, vol. 87, pp. 19-25, 2014.
- [13] T. Hagiwara, S. Fujita, and K. Kizaka, "Assessment of visibility on roads under snow conditions using digital images," in *Proc. 11th International Road Weather Conference*, January 2002.
- [14] L. Xie, A. Chiu, and S. Newsam, "Estimating atmospheric visibility using general-purpose cameras," in *Proc. International Symposium on Visual Computing*, December 2008, pp. 356-367.
- [15] J. P. Andreu, S. Mayer, K. Gutjahr, and H. Ganster, "Measuring visibility using atmospheric transmission and digital surface model," arXiv preprint, arXiv:1505.05286, 2015.
- [16] A. Krizhevsky, I. Sutskever, and G. E. Hinton, "Imagenet classification with deep convolutional neural networks," *Advances in Neural Information Processing Systems*, pp. 1097-1105, 2012.
- [17] A. Palvanov and Y. I. Cho, "VisNet: Deep convolutional neural networks for forecasting atmospheric visibility," *Sensors*, vol. 19, p. 1343, 2019.
- [18] Z. Lei, Z. Guodong, H. Lei, and W. Nan, "The application of deep learning in airport visibility forecast," *Atmos. Clim. Sci.*, vol. 7, pp. 314-322, 2017.
- [19] O. C. Rosangela, L. F. Antonio, A. S. V. Francisco, and R. B. T. Adriano, "Application of artificial neural networks for fog forecast," *J. Aerosp. Technol. Manag.*, vol. 7, pp. 240-246, 2015.
- [20] VGG16 network. [Online]. Available: <https://neurohive.io/en/popular-networks/vgg16/>
- [21] S. Jeevan and L. Usha, "Estimation of visibility distance in images under foggy weather condition," *Int. J. Adv. Comput. Electron. Technol.*, vol. 3, pp. 11-16, 2016.
- [22] V. Vapnik, S. E. Golowich, and A. Smola, "Support vector method for function approximation, regression estimation, and signal processing," *Advances in Neural Information Processing Systems*, pp. 281-287, 1997.
- [23] W. Tian and M. Wang, "Modeling and forecasting method based on support vector regression," in *Proc. Second International Conference on Future Information Technology and Management Engineering*, Dec. 2009.
- [24] G. Gupta and N. Rathee, "Performance comparison of support vector regression and relevance vector regression for facial expression recognition," in *Proc. International Conference on Soft Computing Techniques and Implementations*, 2015, pp. 1-6.
- [25] E. Ying, "Application of support vector regression algorithm in colleges recruiting students prediction," in *Proc. International Conference on Computer Science and Electronics Engineering*, 2012, vol. 2, pp. 173-176.
- [26] X. Mao and J. Yang, "Time series prediction using nonlinear support vector regression based on classification," in *Proc. International Conference on Computational Intelligence for Modelling Control and Automation and International Conference on Intelligent Agents Web Technologies and International Commerce*, 2006.
- [27] N. I. Sapankevych and R. Sankar, "Constrained motion particle swarm optimization and support vector regression for non-linear time series regression and prediction applications," in *Proc. 12th International Conference on Machine Learning and Applications*, 2013, vol. 2.
- [28] J. J. Gerrit, V. D. Burg, and P. J. F. Groenen, "GenSVM: A generalized multiclass support vector machine," *Journal of Machine Learning Research*, vol. 17, pp. 1-42, 2016.
- [29] Visibility readings and weather photos in Hong Kong waters. [Online]. Available: [http://www.hko.gov.hk/vis/vis\\_index.shtml](http://www.hko.gov.hk/vis/vis_index.shtml)
- [30] S. Y. Li, H. Fu, and W. L. Lo, "Meteorological visibility evaluation on webcam weather image using deep learning features," in *Proc. 10th International Conference on Advanced Computer Theory and Engineering*, Jeju Island, South Korea, August 10-13, 2017.

Copyright © 2020 by the authors. This is an open access article distributed under the Creative Commons Attribution License ([CC BY-NC-ND 4.0](https://creativecommons.org/licenses/by-nc-nd/4.0/)), which permits use, distribution and reproduction in any medium, provided that the article is properly cited, the use is non-commercial and no modifications or adaptations are made.



**Wai-Lun Lo** (M'02) received the B.Eng. degree in electrical engineering and the Ph.D. degree from the Hong Kong Polytechnic University, Kowloon, in 1991 and 1996, respectively.

He is currently the Head and Professor of the Department of Computer Science, Chu Hai College of Higher Education. His research interest includes adaptive control, fuzzy systems, application of intelligent control and

machine learning.



**Meimei Zhu** is currently study for her bachelor degree in computer science and technology in Xi'an University of Technology, Xi'an, China. Her research interests focus on image processing. Ms. Meimei Zhu is currently pursuing her Master of Science Degree in School of Computer Science and Engineering, Xi'an University of Technology, Xi'an, China



**Hong Fu** received her Bachelor and Master degrees from Xi'an Jiao tong University in 2000 and 2003, and Ph.D. degree from the Hong Kong Polytechnic University in 2007. She is now an Associate Professor in Department of Computer Science, Chu Hai College of Higher Education, Hong Kong. Her research interests include eye tracking, computer vision, pattern recognition, and artificial intelligence.